A Mobicast Routing Protocol in Underwater Sensor Networks

Yuh-Shyan Chen
Department of Computer Science and Information Engneering
National Taipei University
Taipei, Taiwan, R. O. C.
Email: yschen@mail.ntpu.edu.tw

Yun-Wei Lin and Sing-Ling Lee
Department of Computer Science and Information Engneering
National Chung Cheng University
Chia-Yi, Taiwan, R.O.C.
Email: jyneda@gmail.com, singling@cs.ccu.edu.tw

***Abstract*—A mobicast, or called as mobile geocast, problem in three-dimensional (3D) underwater sensor networks (USNs) is investigated in this paper, which aims to overcome the hole problem and minimizes the energy consumption of the sensor nodes while maximizing the data collection. In this work, all underwater sensor nodes are randomly distributed in a 3D underwater environment in the sea to form a 3D USN. Considered a mobile sink or an AUV (autonomous underwater vehicle), all possible sensor nodes near to the AUV form a 3D geographic zone (called as 3D zone of reference or 3D ZOR). The AUV travels a user-defined route and continuously collects data form sensor nodes within a series of 3D ZORs at different time. The main problem is how to efficiently collect data from sensor nodes within a 3D ZOR while those sensor nodes are usually in sleep mode for a long period of time. The routing protocol relies on two phases; the first phase is to collect data form sensor nodes within a 3D ZOR, and the second phase is to wake up those sensor nodes in the next 3D ZOR to be queried while trying to avoid topology holes. To save power, only sensor nodes in a 3D ZOR are notified to enter the active mode in order to deliver sensed results to the AUV. To consider the characteristics of USNs, a new mobicast routing protocol is developed in 3D USNs. The key design challenge is to develop a power-saving mobicast protocol in 3D USNs to overcome the unpredictable 3D hole problem. An "apple slice" technique is used to build multiple segments to surround a hole and to assure routing path continuity. Finally, performance analysis is derived and simulation results illustrate the performance improvement in successful delivery rate and power consumption.**

Keywords: underwater sensor network, mobicast, geocast, multicast,routing.

I. Introduction

Underwater sensor networks (USNs) consist of number of sensor nodes which are equipped with acoustic transceivers that enable them to communicate with each other to perform collaborative sensing tasks over a given area [1] from shallow water and seabed. USNs have many potential applications in ocean monitoring, such as current flow and oil pollution monitoring. The power consumption issue are mainly focused on USNs [1]. Acoustic communication in the ocean encounters a longer propagation delay. The location of sensor nodes in the ocean is usually changed caused by the ocean current. The USN is thus with the changeable topology over time. In addition, the network fragmentation or hole problem is occurred because that there is no uniform distribution of underwater sensor nodes and the ocean current.

In this paper, a new multicast routing paradigm called a "mobicast" is proposed in 3D USNs. A geographic zone, called as 3D zone of relevance (3D ZOR), is prescribed by an AUV (autonomous underwater vehicle) [2]. The AUV acts as a mobile sink and nearly collects the sensed data from sensor nodes. The spatiotemporal character of a mobicast is to collect the sensed data from sensor nodes that will be present at time t in the 3D ZOR. Assumed that an AUV travels a circle path around a given observed area. The AUV constructs a series of 3D ZORs over different intervals (t_{start}, t_{end}), and only sensor nodes located in the 3D ZOR at the time interval (t_{start}, t_{end}) must wake up to send sensed data to the AUV. After the AUV left the 3D ZOR, sensor nodes within this 3D ZOR can switch to sleep mode for power saving. It is observed that the 3D ZOR is evolved and continuously moves with the AUV over time. Regarding existing routing protocols in 3D USNs, Pompili *et al.* [3] proposed a unicast routing algorithm in 3D underwater sensor networks to allow each node to select its next hop with the highest successful delivery rate under the minimum energy consumption. This protocol focus on providing unicast routing in 3D networks. The routing requirement which considers the temporal and spatial issues at the same time to provide spatiotemporal multicast routing in 3D underwater sensor networks needs to be further investigated.

To successfully collect sensed data, sensor nodes in 3D ZOR must be waken up to wait for the arrival of the AUV. Wang [2] proposed an data collection solution in the underwater environment. However, this protocol does not consider to collect data from sensor nodes which may usually stay in sleep mode for a long period of time. An AUV cannot successfully receive the sensed data in time if sensor nodes in the 3D ZOR are still in sleep mode. A sensor node may be not woke up by a waking up message sent from the AUV when the AUV is near to the sensor node because the waking up message may fail to deliver due to the hole problem and the ocean current effect. To consider the characteristics of USNs, a distributed mobicast routing protocol in 3D USNs is proposed to deliver mobicast messages for waking up all sensor nodes within a 3D ZOR at time t for data collection. This is the first result to develop a mobicast routing protocol in USNs. The key design challenge is to develop a power-saving mobicast protocol in 3D USNs to overcome the unpredictable 3D hole problem. A apple-slice scheme of the mobicast protocol is proposed to solve the unpredictable 3D hole problem. Finally, simulation results illustrate the performance improvement in successful delivery rate and power consumption.

The rest of this paper is organized as follows. Section II presents the challenges and basic ideas. section III presents the new mobicast routing protocol. Performance analysis is discussed in section IV. Finally, section V concludes this paper.

II. Preliminaries

This section presents the system model and basic idea. The contribution and the application examples are also introduced.

A. System Model

In this work, sensor nodes are randomly deployed in the ocean. Sensor nodes are drifted by ocean currents. We assume each sensor node can know its location by range-based localization techniques [4]. Fig. 1 shows the architecture in this work. The AUV travels along a user-defined route with a constant velocity and collects sensed data from sensor nodes in a series of 3D ZORs. The AUV should accomplish the route before a user-defined response time, and then the AUV returns to a control station and reports the collected data. Sensor nodes usually stay at sleep mode for power saving. If the AUV wants to successfully collect sensed data, sensor nodes should be waked up first. Since the AUV should accomplish the route before the user-defined response time, the AUV cannot stop its movement to wait for a sensor node to wake up. Hence, sensor nodes should be waked up first while the AUV is approaching. This is, sensor nodes located at right "place" and at right "time" should be waked up to send sensed data.

In the following, we define 3D ZOR_t (3D zone of relevance) and 3D ZOF_{t+1} (3D zone of forwarding). Let N_i denote as the ID of a sensor node, where $i = \{1, 2, ..., i, i+1, ..., n\}$ throughout this paper. The 3D ZOR_t is a geographic zone created by the AUV at time t to indicate which sensor node should send the sensed data to the AUV. A formal definition of 3D ZOR_t is given.

Definition 3D $\mathbf{ZOR_t}$ or $\mathbf{ZOR_t^3}$ (3D zone of relevance): Given an AUV, 3D ZOR_t is a 3D spherical region determined by AUV at time t, such that sensor node N_i must transmit the sensed data to AUV at time t, where N_i is located within the 3D ZOR_t. The center location of 3D ZOR_t is the same with the location of AUV, moving at the same speed as AUV, and toward the same direction with AUV.

Fig. 1 shows an example of 3D ZOR_t^3, where the time is from t to $t+1$. The AUV collects sensed data from sensor nodes located in ZOR_t^3 at time t. To continuously collect sensed data from all sensor nodes in the USN, a new ZOR_{t+1}^3 should be created for data collection at time $t+1$. Sensor nodes usually stay at sleep mode for power saving. To wake up those sensor nodes within ZOR_{t+1}^3 in advance, a "hold and forward" zone is used. The hold and forward zone is an overlapping area between ZOR_t^3 and ZOR_{t+1}^3 as shown in Fig. 2(a). Sensor nodes located in the hold and forward zone should wake up all sensor nodes in ZOR_{t+1}^3 by delivering the mobicast message. Then the AUV can collect sensed data from sensor nodes in ZOR_{t+1}^3 at time $t+1$. However, sensor nodes may be drifted away by ocean current and that causes the hole problem. The mobicast message cannot not be delivered to some sensor nodes within ZOR_{t+1}^3 due to the hole problem. Some sensor nodes can not be waked up to prepare for sending data. Fig. 2(b) shows an example of mobicast with the hole problem. At time $t+1$, a partial sensor nodes in ZOR_{t+1}^3 are

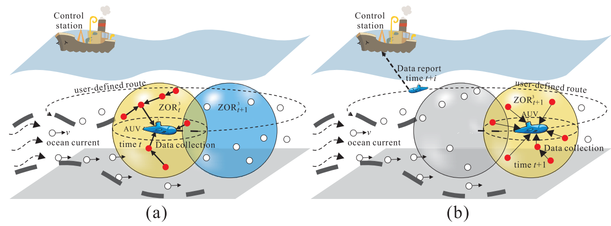

Fig. 1. An AUV collects data form sensor nodes in (a) ZOR_t^3 at time t (b) ZOR_{t+1}^3 at time $t+1$.

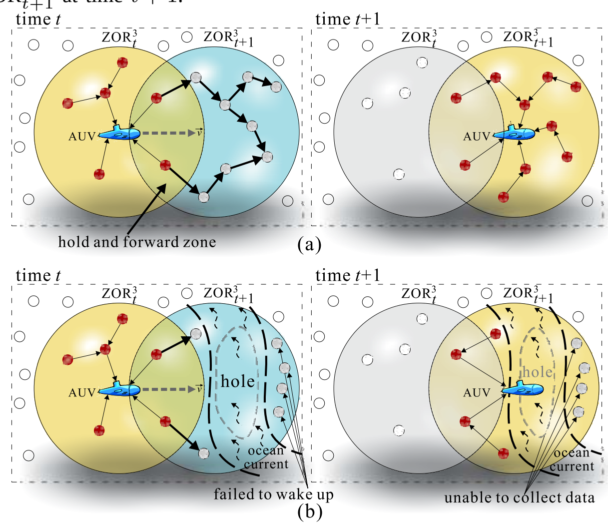

Fig. 2. (a) Successful data collection (b) AUV failed to collect data form part sensor nodes due to ocean current.

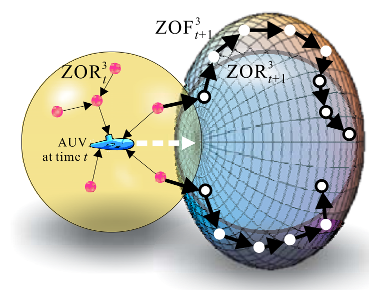

Fig. 3. ZOF_{t+1}^3 is oblate spheroidal region and covers ZOR_{t+1}^3.

failed to be waked up due to the hole problem. The AUV can not collect sensed data from those sensor nodes in sleep mode. To overcome the hole problem, a zone of forwarding 3D ZOF_{t+1} is created by the AUV at time t. The 3D ZOF_{t+1} is a geographic zone created by the AUV at time t to indicate which sensor node should deliver the mobicast message for waking up sensor nodes within ZOR_{t+1}^3. A formal definition of 3D ZOF_{t+1} is given.

Definition 3D $\mathbf{ZOF_{t+1}}$ or $\mathbf{ZOF_{t+1}^3}$ (3D zone of forwarding): Given an AUV, 3D ZOF_{t+1} is a 3D oblate spheroidal region determined by AUV at time t, such that each sensor node N_i within the 3D ZOF_{t+1} has the responsibility of forwarding the mobicast message to sensor nodes within 3D ZOR_{t+1}.

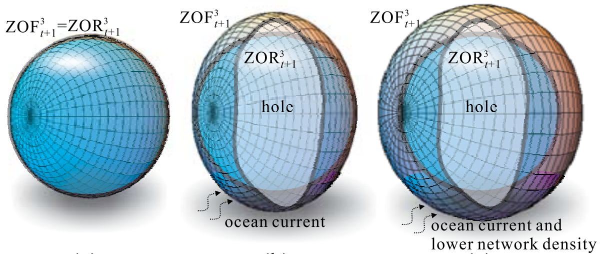

(a) (b) (c)

Fig. 4. ZOF$^3_{t+1}$ expands to cover the hole based on the network density and the ocean current.

Fig. 3 shows an example of 3D ZOF$_{t+1}$. ZOF$^3_{t+1}$ always covers ZOR$^3_{t+1}$ and the alternative routing paths can be discovered in ZOF$^3_{t+1}$ to deliver the the mobicast message. The hole problem is solved. However, since the battery power in USNs is a valuable resource, sensor nodes within ZOF$^3_{t+1}$ should be carefully chosen for the mobicast message delivery. In a 3D ZOF$_{t+1}$, there are multiple routing paths which can be used to deliver the mobicast message. With the consideration of the direction of current flow, the successful delivery rate is different on different routing paths. We discuss how to select routing paths to achieve the highest successful delivery rate or save power in the next section.

B. Basic Idea

To ensure that sensor nodes within ZOR$^3_{t+1}$ can be waked up for sensed data delivery, two steps are used. The first step is to determine the size of ZOF$^3_{t+1}$. A large size of ZOF$^3_{t+1}$ can overcome the hole problem and achieve higher successful delivery rate but consumes much power. On the other hand, a small size ZOF$^3_{t+1}$ may not overcome the hole problem. Therefore, the size of ZOF$^3_{t+1}$ should be carefully considered. To overcome the 3D hole in ZOR$^3_{t+1}$, the drifted distance of sensor nodes is the major concern. ZOF$^3_{t+1}$ should be capable of covering a sensor node even if the sensor node is drifted by the ocean current. Therefore, the size of ZOF$^3_{t+1}$ is determined by the velocity of ocean currents and the network density. Fig. 4 (a) illustrates the size of ZOF$^3_{t+1}$ is equal to the size of ZOR$^3_{t+1}$if there is no ocean current in ZOF$^3_{t+1}$. If there exists an ocean current in ZOF$^3_{t+1}$, the size of ZOF$^3_{t+1}$ is enlarged to cover the drifted sensor nodes based on the velocity and direction of the ocean current as shown in Fig. 4 (b). If the network density is getting lower in ZOF$^3_{t+1}$, ZOF$^3_{t+1}$ expands to a larger size to cover more sensor nodes for route discovery, as shown in Fig. 4 (c).

The second step determines how many sensor nodes are used to deliver the mobicast message. Two algorithms, A and B, are proposed. Algorithm A uses all sensor nodes within 3D ZOF$^3_{t+1}$ to deliver the mobicast message to achieve the highest successful delivery. Algorithm B aims to keep a high successful delivery rate and reduce the power consumption as much as possible. With the consideration of the ocean current, the successful delivery rate within different parts of ZOF$^3_{t+1}$ are different. To keep a high successful delivery rate and save power, the only sensor nodes which are necessary to wake up are those nodes belonging to those parts of ZOF$^3_{t+1}$ with a high successful delivery rate. To divide a ZOF$^3_{t+1}$ into several parts, we use a simple concept – slice apple, as shown in Fig. 5. We slice a ZOF$^3_{t+1}$ into m several identical parts. We called each part as a *segment*.

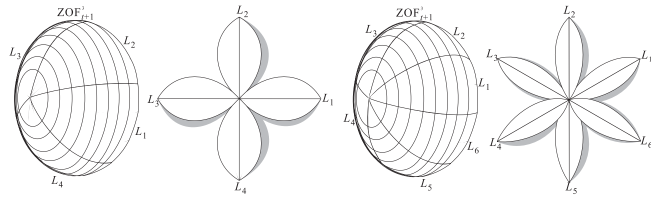

(a) (b)

Fig. 5. ZOF$^3_{t+1}$ is split into (a) four segments and (b) six segments.

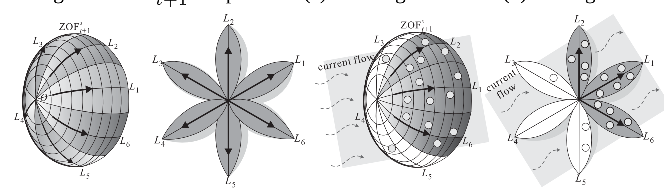

(a) (b)

Fig. 6. Messages delivery using (a) all segments (b) only segments L_1, L_2, and L_6.

Definition L_i (**segment**)**:** Given an 3D oblate spherical ZOF$^3_{t+1}$, the geographic location of sensor nodes in the oblate sphere can be indicated as area "L". The area L can be divided into m identical parts. We called the each part of L as a segment L_i, where $i = 1, 2, ..., m$.

Fig. 5 (a) and (b) show that the ZOF$^3_{t+1}$ is split into four segments and six segments, respectively. The key idea of this work is to use those sensor nodes in those segments to deliver the mobicast for waking up sensor nodes in ZOR$^3_{t+1}$. Algorithm A is proposed to achieve the highest successful delivery rate. All sensor nodes are used to deliver the mobicast message as shown in Fig. 6 (a). Algorithm B aims to keep a high successful delivery and save power. The only segments with a higher successful delivery rate are used to deliver the mobicast message as shown in Fig. 6 (b). A segment L_i with a higher successful delivery rate implies that the direction of message delivery is similar with the direction of current flow. This is because sensor nodes are drifted in the same direction with the same velocity; hence, the topology does not change so quickly and links between sensor nodes have a longer life-time. Finally, the size of a segment can adaptively expand based on the real-time velocity and direction of the ocean current in ZOF$^3_{t+1}$. Fig. 7 (a) shows the size of segment L_1 is small if the velocity of the ocean current in ZOF$^3_{t+1}$ is slow and fig. 7 (b) shows the size of segment L_1 is large if the velocity of the ocean current in ZOF$^3_{t+1}$ is fast. The detailed algorithm of the mobicast routing protocol is given in the next section.

III. Mobicast Routing Protocol

In this section, we describe how an AUV collects sensed data from sensor nodes with our mobicast protocol. Our mobicast protocol is split into two phases, 3D ZOR$_t$ creation phase and 3D ZOF$_{t+1}$ creation phase. In 3D ZOR$_t$ creation phase, AUV creates the ZOR^3_t at time t to collect sensed data and delivers a mobicast message to wake up sensor nodes which will be present at time $t + 1$ in ZOR$^3_{t+1}$. In 3D ZOF$_{t+1}$ creation phase, the ZOF$^3_{t+1}$ is created with a proper size to cover the potential hole; meanwhile, ZOF$^3_{t+1}$ is split into several segments for the mobicast message delivery. The detailed operation is developed as follows.

A. 3D ZOR_t creation phase

Sensor nodes located within ZOR_t^3 should send the sensed data to AUV. To collect sensor data from all sensor nodes in the USN, AUV should continuously create a series ZOR_t^3 at different time t. The procedure to create the ZOR_t^3 is given herein.

S1. AUV acquires the location (x_A, y_A, z_A) based on range-based localization techniques [4].

S2. To collect sensed data from sensor node, AUV creates the ZOR_t^3 by the equation $Z_t(N_i) = (x_i - x_A)^2 + (y_i - y_A)^2 + (z_i - z_A)^2 - R^2 = 0$, where R is the radius of ZOR_t^3, (x_i, y_i, z_i) is the location of a sensor node N_i and (x_A, y_A, z_A) is the center of ZOR_t^3. R is defined by a user to indicate a expected range for data collection. A sensor node N_i should send the sensed data to the AUV if $Z_t(N_i) \leq 0$ which implies sensor node N_i is located within ZOR_t^3.

S3. AUV broadcasts the mobicast control packet $P_m(N_i, Z_t(N_i), m_b, r, \overrightarrow{v_A})$, where $Z_t(N_i)$ describes the region of ZOR_t^3, m_b is the mobicast message, r is the radius of hold and forward zone, and $\overrightarrow{v_A}$ is velocity of AUV. After AUV broadcasting the P_m, 3D ZOF_{t+1} creation phase is executed.

B. 3D ZOF_{t+1} creation phase

To wake up sensor nodes located in the ZOR_{t+1}^3, ZOF_{t+1}^3 is necessary to create at time t. Sensor nodes within ZOF_{t+1}^3 should deliver the mobicast message to wake up those sensor nodes will be present within ZOR_{t+1}^3. Two algorithms, A and B, are proposed to deliver the mobicast message. Algorithm A uses all sensor nodes within ZOF_{t+1}^3 to deliver the mobicast message. Algorithm B divides the ZOF_{t+1}^3 into m identical segments and uses the only segments with a higher successful delivery rate to deliver. We first present algorithm A as follows.

S1. To deliver the mobicast message for waking up sensor nodes in ZOR_{t+1}^3, ZOF_{t+1}^3 is created by $F_{t+1}(N_i) = \frac{(x_i - x_F)^2 + (y_i - y_F)^2}{a^2} + \frac{(z_i - z_F)}{c^2} - 1 = 0$, where (x_F, y_F, z_F) is the center of ZOF_{t+1}, a is the equatorial radius of ZOF_{t+1}^3, and c is the polar radius of ZOF_{t+1}^3. The initial size of ZOF_{t+1}^3 is determined based on the network density and the current flow in ZOR_t^3. ZOF_{t+1}^3 should be able to tolerate the current flow and cover the hole; therefore, the size of ZOF_{t+1}^3 is expanded with the speed of the current flow. Let nd_t denote as the network density within ZOR_t^3, nd_{avg} denote as the average network density, and $\overrightarrow{C}$ denote as the velocity of current flow. The value of $a = R \times (1 + \frac{\overrightarrow{a} \cdot \overrightarrow{C}}{|\overrightarrow{C}|})$ and $c = R \times (1 + \frac{\overrightarrow{c} \cdot \overrightarrow{C}}{|\overrightarrow{C}|})$ if $nd_t \geq nd_{avg}$. Otherwise, $a = \frac{nd_{avg}}{nd_t} \times R \times (1 + \frac{\overrightarrow{a} \cdot \overrightarrow{C}}{|\overrightarrow{C}|})$ and $c = \frac{nd_{avg}}{nd_t} \times R \times (1 + \frac{\overrightarrow{c} \cdot \overrightarrow{C}}{|\overrightarrow{C}|})$ if $nd_t < nd_{avg}$. The condition $nd_t < nd_{avg}$ means that the network density is getting lower and ZOF_{t+1}^3 should expand to a larger size.

S2. To wake up sensor nodes in ZOR_{t+1}^3, sensor nodes located in a ”hold and forward zone” should deliver the mobicast message through sensor nodes in ZOF_{t+1}^3. The hold and forward zone is a overlap between ZOR_t^3 and ZOR_{t+1}^3. The radius of the hold and forward zone is r, which is defined by a user.

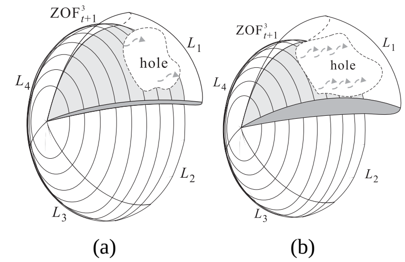

Fig. 7. The segment adaptively expands to cover the hole.

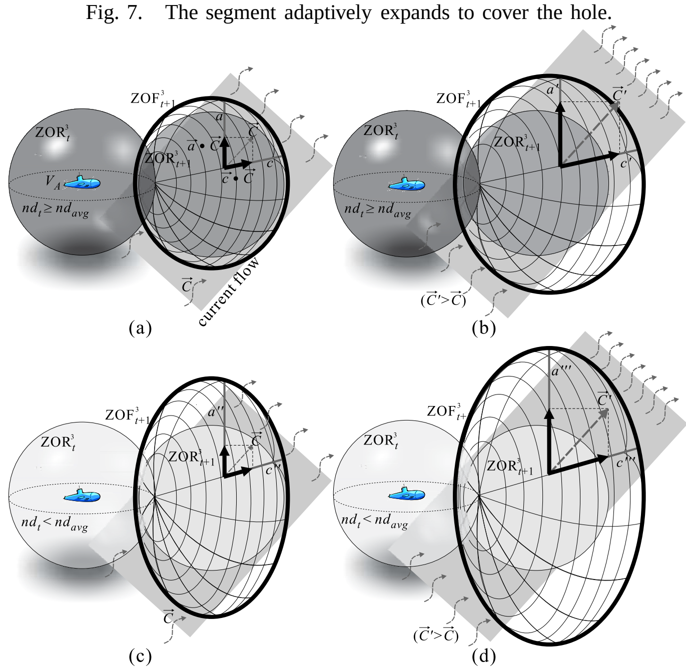

Fig. 8. Various size of ZOF_{t+1}^3 based on diffetent network density and current flows: (a) the high density and the slow current (b) the high density and the fast current (c) the low density and the slow current (d) the high density and the fast current.

S3. To achieve high successful delivery rate, Algorithm A uses all sensor nodes in ZOF_{t+1}^3 to deliver the mobicast message.

Step 1 creates various sizes of ZOF_{t+1}^3 to cover the hole based on the network density and the velocity of current flow in ZOR_t^3 as shown in Fig. 8. Observe that it may not accurately predict the size ZOF_{t+1}^3 by the network density nd_t and the velocity of current flows $\overrightarrow{C}$ in ZOR_t^3; therefore, a real-time size adjustment scheme for ZOF_{t+1}^3 is proposed in algorithm B.

Algorithm B aims to save power and keep a high successful delivery rate. The ZOF_{t+1}^3 is sliced into m segments, and only those segments with a higher delivery rate are used to deliver the mobicast message. To find which segments are required to deliver the mobicast message, we have the lemmas below.

Lemma 1: Given a 3D oblate spheroidal ZOF_{t+1}^3 and a vector of current flow $\overrightarrow{C}$; then we know the optimum segment quantity $m = \left\lceil \frac{2\pi a}{\overrightarrow{s_i^{\delta}} \cdot \overrightarrow{C}} \right\rceil$, where $\overrightarrow{s_i^{\delta}}$ is an orthogonal vector of $\overrightarrow{s_i}$, where $\overrightarrow{s_i}$ is the message delivery direction in segment L_i.

Proof: A segment with a larger size can tolerate a stronger current flow. This is because sensor nodes may not easily

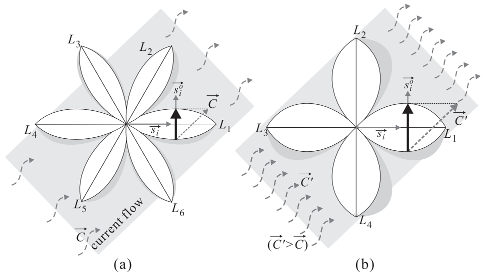

Fig. 9. The ocean current and the segment quantity.

drift out of a large segment. A routing path could be easier to establish; therefore, the delivery rate is usually high in a segment with a large size. On the other hand, a segment with a large size involves more nodes to deliver messages and consumes much power. Hence, to find a suitable size of a segment is an important issue. A segment can tolerate a stronger current flow means that a sensor node does not drift out of the segment during the time interval $(t, t+1)$. Since the delivery direction is $\overrightarrow{s_i}$, $\overrightarrow{s_i^o}$ is the direction which a node drifts out of the segment. The distance which a node drifts during the time $(t, t+1)$ is $\overrightarrow{s_i^o} \cdot \overrightarrow{C} \times (t-t+1)$. This is, if the width of a segment L_i larger than $\overrightarrow{s_i^o} \cdot \overrightarrow{C}$, then this segment can tolerate the current flow. Since a segment L_i has a arc length with $\overrightarrow{s_i^o} \cdot \overrightarrow{C}$ and the the arc length of a ZOF$^3_{t+1}$ is $2\pi a$, then we can know the optimum segment quantity m is $\left\lceil \frac{2\pi a}{\overrightarrow{s_i^o} \cdot \overrightarrow{C}} \right\rceil$. ■

A segment with a suitable size can tolerant the current flow. Fig. 9 shows that the size of segments is determined according to the velocity of ocean current.

Lemma 2: Assume that the successful communication rate is p. Given a successful prediction probability $(1-\alpha)$; then the minimum node quantity for getting the largest node efficiency is $n_m = (50Z_{\frac{\alpha}{2}}\sqrt{p(1-p)})^{\frac{2}{3}}$.

Proof: To find the minimum node quantity for getting the largest node efficiency, we should first know the failed delivery rate when how many sensor nodes are used to deliver a message. Let n denote as node quantity which means there are n sensor nodes to be involved for messages delivery. An error rate function $E(n) = \frac{Z_{\frac{\alpha}{2}}\sqrt{p(1-p)}}{\sqrt{n}}$ derived from Z-distribution [5] can be used to predict the failed delivery rate when there are n sensor nodes to be involved to deliver, where $Z_{\frac{\alpha}{2}}$ is a z-value which can find from a Z-distribution table [5]. To efficiently deliver the mobicast message, the *node efficiency* should be large than or equal to 1%. The node efficiency represents how much error rate is reduced while one sensor node is added to deliver. The first order differential of $E(n)$ is $E'(n)$ which can describe the node efficiency, where $E'(n) = -\frac{Z_{\frac{\alpha}{2}}\sqrt{p(1-p)}}{2}n^{-\frac{3}{2}}$. To find n_m, we let $E'(n) = -1\%$. Then we know $n_m = (50Z_{\frac{\alpha}{2}}\sqrt{p(1-p)})^{\frac{2}{3}}$. ■

Lemma 3: Given a 3D oblate spheroidal ZOF$^3_{t+1}$ and the minimum required node quantity n_m. Then the required segment quantity L_R is $\frac{\frac{n_m}{nd_t}}{\frac{\frac{4}{3}\pi a^2 c}{m}}$.

Proof: The required segment quantity L_R can be derived from the total required volume. The total required volume can be calculated by $\frac{n_m}{nd_t}$, and the volume of each segment is $\frac{\frac{4}{3}\pi a^2 c}{m}$, then we know the required segment quantity $L_R = \frac{\frac{n_m}{nd_t}}{\frac{\frac{4}{3}\pi a^2 c}{m}}$. ■

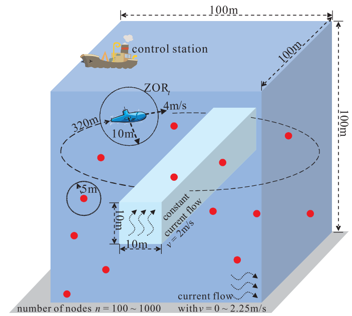

Fig. 10. The simulation environment and parameters.

Algorithm B is presented as follows. Steps 1 and 2 of algorithm B are the same as algorithm A. We describe algorithm B from step 3 below.

S3'. Segments with higher delivery rate are identified in this step. To achieve high successful delivery rate and power saving , ZOF$^3_{t+1}$ is divided into m identical segments according to Lemma 1. The only segments with a high successful delivery rate should deliver the mobicast message. A segment has a higher successful delivery rate if the delivery direction of the segment $\overrightarrow{s_i}$ is similar to the direction of current flow $\overrightarrow{C}$. So let a segment with a shorter defer time to deliver if $\overrightarrow{C} \cdot \overrightarrow{s_i}$ is larger. A larger $\overrightarrow{C} \cdot \overrightarrow{s_i}$ implies that the delivery direction is more similar to the direction of current flow, then the successful delivery rate is higher.

S4'. Sensor node N_i should deliver the mobicast message if $F_{t+1}(N_i) \leq 0$. $F_{t+1}(N_i) \leq 0$ implies N_i is located within ZOF$^3_{t+1}$. When sensor node N_i in segment L_i receives P_m sent from a neighboring segment, L_{i+1} or L_{i-1}, the sensor node immediately broadcast P_m until the required segment quantity L_R is satisfied, where L_R is $\frac{\frac{n_m}{nd_t}}{\frac{\frac{4}{3}\pi a^2 c}{m}}$ according to Lemma 3.

S5' The size of a segment can adaptively adjust since the initial size of ZOF$^3_{t+1}$ may not accurately predict. N_i replaces the parameters in step 1 of algorithm A with the real-time current flow $\overrightarrow{C}$ in segment L_i and network density nd_{t+1} to acquire the new radius $a\prime$ and $c\prime$. With $a\prime$ and $c\prime$, ZOF$^3_{t+1}$ has the proper size to tolerate the ocean current.

IV. Simulation Results

Our paper presents a mobicast routing protocol in underwater sensor networks. The protocols are mainly implemented using the ns2 simulator and Aqua-Sim emulator. Because our mobicast protocol is the first mobicast result in USNs, we simulate our mobicast protocol to observe results when the mobicast message is delivered using 100% segments, $\frac{L_R}{m}\%$ segments, and 30% segments. Algorithm A using 100% segments is denoted as 100% segments. The message delivery using 30% segments is denoted as 30% segments. Algorithm B uses the only sensor nodes in $\frac{L_R}{m}\%$ segments to deliver messages, which is denoted as L_R/m% segments. The simulation environment is shown as Fig. 10. The system parameters are given below. To discuss the effect of the network density (ND) of a USN, our simulator considers a 3D cubic region with a size of 100 x 100 x 100 units with various numbers of

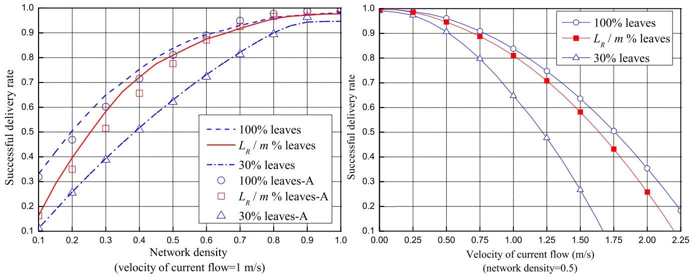

(a) (b)

Fig. 11. Performance of successful delivery rate vs. (a) network density (b)current's velocity.

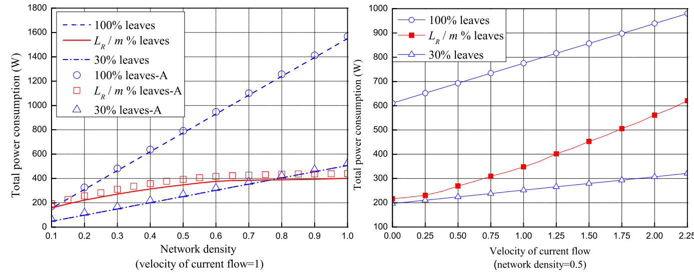

(a) (b)

Fig. 12. Performance of power consumption vs. (a) network density (b) current's velocity.

nodes, ranging from 100 to 1000. The communication range of a sensor node and the AUV are 5 units and 10 units, respectively. The radius of ZOR$_t^3$ is 10 units. The velocity of AUV is constant 4 unit/sec. The velocity of current flow (v) is from 0 to 2.25 unit/sec. The time interval between time t and $t+1$ is 5 seconds. We set the power consumption parameters based on the underwater acoustic modem, UMW1000, from LinkQuest. The power consumption on transmission mode, receive mode, and sleep mode are 2 Watts, 0.75 Watts, and 8 mW, respectively. It is noted that 100% segments-A, 30% segments-A, and L_R/m% segments-A are denoted as the analyzed results derived from the mathematics analysis. The mathematics analysis does not present due to the pages limitation. The performance metrics to be observed are:

- The *successful delivery rate* (SDR) is the number of nodes located in ZOR$_{t+1}^3$ which can successfully receive the mobicast messages and wake up, divided by the total number of nodes in ZOR$_{t+1}^3$.
- The *power consumption* (PC) is the total power consumption that all sensor nodes consumed.

It is worth mentioning that an efficient mobicast protocol in a USN is achieved with a high SDR and low PC. In the following, we illustrate our simulation results for *successful delivery rate* (SDR) and *power consumption* (PC) from several aspects.

A. Successful delivery rate (SDR)

Fig. 11 (a) shows the observed SDR under various NDs. The higher the ND is, the higher the SDR will be. It was observed that SDR was very low when ND< 0.2 because several sensor nodes were totally isolated under very low density. The SDR of L_R/m% segments is closed to 100% segments when ND> 0.6. This is because the delivery uses L_R/m% segments with a higher successful delivery rate. The SDR of 30% segments is lower because sensor nodes in 30% segments are not enough to deliver messages under the low network density. Fig. 11 (b) shows the observed SDR under various v. The delivery using 100% segments can achieve maximum SDR since all sensor nodes in ZOF$_{t+1}^3$ are involved to deliver the mobicast message. The SDR of L_R/m% segments is closed to 100% segments under various v because algorithm B considered the effect of current flow and chose L_R segments with a higher successful delivery rate to deliver. The SDR of 30% segments drops quickly when the v is higher because only 30% segments are not sufficient to deliver the mobicast message under higher v.

B. Power consumption (PC)

Fig. 12 (a) shows the observed PC under various NDs. The higher the ND is, the higher the PC will be. This is because more and more nodes are involved to deliver messages. Compared to the delivery using 100% segments, the delivery using 30% segments reduces about 70% power consumption. Observe that, the PC of L_R/m% segments under high density is lower than the PC of 30% segments. This is because the required segment quantity L_R is lower than 30% segments when the ND is higher than 0.8. Fig. 12 (b) shows the observed PC under various v. The higher the v is, the higher the PC will be. This is because that the size of ZOF$_{t+1}^3$ is larger when the velocity of current flow v is higher. The curve of the PC of L_R/m% segments is lower than that of 100% segments under various velocity of current flow v. The PC of L_R/m% segments increases quickly when the velocity of current flow v is higher. This is because the size of each segment is large to keep the successful delivery rate when v is high.

V. Conclusion

In this paper, we present a mobicast routing protocol to dynamically estimate the accurate ZOF$_{t+1}^3$ to successfully deliver mobicast messages to wake up all sensor nodes in ZOR$_{t+1}^3$ for data collection. The hole problem and the ocean current effect are also taken into consideration. Finally, the simulation results illustrated our performance achievements in terms of successful delivery rate and power consumption.

VI. Acknowledgements

The authors would like to thank the anonymous reviewers and the editors for the valuable suggestions to improve this paper. This research was supported by the National Science Council of the R.O.C. under grant NSC-97-2221-E-305-005.

References

[1] I. F. Akyildiz, D. Pompili, and T. Melodia, "The State of Art in Protocol Research for Underwater Acoustic Sensor Networks," *ACM International Workshop on Underwater Networks (WUWNet)*, vol. 11, pp. 11–22, 2006.

[2] J. Wang, D. Li, M. Zhou, and D. Ghosal, "Data Collection with Multiple Mobile Actors in Underwater Sensor Networks," *International Conference on Distributed Computing Systems Workshops*, pp. 216–221, June 2008.

[3] D. Pompili and T. Melodia, "Three-dimensional Routing in Underwater Acoustic Sensor Networks," *ACM International Workshop On Performance Evaluation of Wireless Ad Hoc, Sensor, and Ubiquitous Networks (PE-WASUN)*, pp. 834–842, Oct. 2005.

[4] A. Y. Teymorian, W. Cheng, X. C. L. Ma and, X. Lu, and Z. Lu, "3D Underwater Sensor Network Localization," *IEEE Transactions on Mobile Computing*, vol. 8, pp. 1610–1621, Dec. 2009.

[5] S. Amari and H. Nagaoka, "Methods of Information Geometry," *Oxford University Press*, ISBN 0-8218-0531-2, 2000.